International Journal of New Horizons in Physics

http://dx.doi.org/10.18576/ijnhp/030101

Studies on Atmospheric Non-Thermal Plasma Jet Device

H. A. El-sayed, T. M. Allam and K. M. Ahmed.*

Plasma and Nuclear Fusion Dept., Nuclear Research Center, Atomic Energy Authority, Egypt.

Received: 21 Feb. 2015, Revised: 22 Mar. 2015, Accepted: 24 Mar. 2015.
Published online: 1 Jan. 2016.

Abstract: This paper presents results of experimental studies carried out with atmospheric pressure non-thermal plasma jet, ANPJ, device energized by a low-cost Neon power supply of (10 kV, 30 mA, and 20 kHz). The discharge takes place by using compressed Air and N_2 gas separately with a flow rate from 3 to 25 L/min and charging voltage of 6 kV. All the results are taken during a period time of 100 µs. The excitation electron temperature has been measured using the photomultiplier tube, PMT, with two different wavelength filters of 460 and 500 nm. The plasma jet device operational time effect on the temperature of the device components has been studied by using a thermometer. Scanning electron microscope, SEM, images were taken to visualize the changes in the surface of Polyethylene terephthalate, PET before and after treatment with N_2 and Air Plasma Jet separately, and at optimum operation condition of plasma jet device.

Keywords: Plasma jet, excitation electron temperature, scanning electron microscope

1 Introduction

Atmospheric pressure plasma (APP) overcomes the disadvantages of vacuum operation. A general recipe for obtaining non-thermal plasmas is the reduction of the discharge size and/or its duration, and working at low excitation frequency [1]. The most used devices for generating atmospheric pressure non-thermal plasmas are atmospheric pressure plasma jet, plasma needle, plasma pencil, miniature pulsed glow-discharge torch, one atmosphere uniform glow-discharge plasma, resistive barrier discharge and dielectric barrier discharge [2].

One of the attractive features of non-thermal atmospheric pressure plasmas is the ability to achieve enhanced gas phase chemistry without the need for elevated gas temperatures. This attractive characteristic recently led to their extensive use in applications that require low temperatures, such as in material processing and in biomedical applications [3-6].

Previous experimental results of the atmospheric pressure non-thermal plasma jet device, under consideration, showed that a maximum plasma jet length of 14 mm and 7 mm is detected for N_2 and Air respectively at flow rate of 12 L/min [7-8].

The use of cold plasmas for materials processing has gained acceptance in a large number of technologies, from metallurgy to manufacturing of computer chips, and covers a wide variety of materials, including metals, semiconductors, and polymers. Most applications of cold plasmas based on plasma enhanced chemical processing focus on treating solid surfaces, film deposition, modification of surfaces, and etching of surface layers. Cold plasmas are also used to synthesize gases or liquids as final products.

The purpose of our study is to investigate the electronic excitation temperature of plasma jet, the components temperature of plasma jet device as a function of operation device time and study the effect of plasma jet treatment time on the surface of PET substrate.

2 Electrode System and Assembly of ANPJ

The electrode system of the ANPJ (7-8) consists of two parallel aluminum disks, the cathode with thickness of 3 mm and 21 mm diameter and the anode with the same thickness and 9 mm diameter. The two electrodes are separated by three Teflon disks each of 0.5 mm thickness and 21 mm diameter as an insulator. The two electrodes and the insulator are stacked together and drilled at the center to have a hole of 800 µm diameter. The device is energized by a low cost Neon power supply of (10 kv, 30 mA, and 20 kHz). As the gas is fed to the electrode system through the hole, a well-defined plasma jet expands into ambient air and elongates as a function of gas flow rate. The system operates with nitrogen and compressed air with flow rate ranging from 0 to 25 L/min and input voltage of 6 KV.

A photomultiplier tube (PMT) with double filters of

*Corresponding author e-mail: hanaa.elshamy@yahoo.com

wavelength 460 and 500 nm is used to measure the electronic excitation temperature. These two filters are put perpendicular to the jet flame at 20 mm distance from the cathode surface. Figure 1 shows the schematic diagram of the electrode system and the PMT with the double filters.

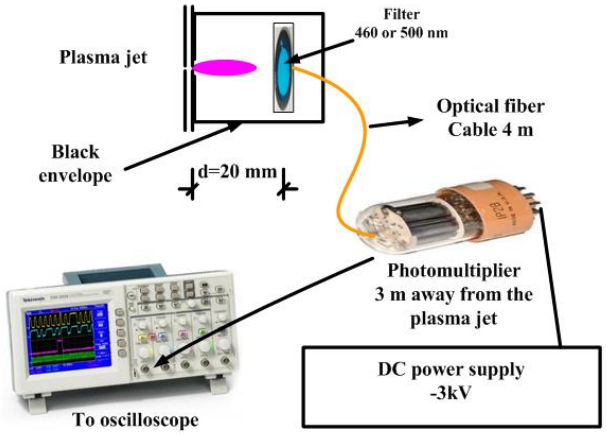

Fig. 1 Arrangement of the setup used for using PMT with double filters.

3 Experimental Results

3.1 The electronic excitation temperature

The electronic excitation temperature, KT_{exc} is calculated by some N OES (Nitrogen optical emission spectroscopy) lines, which can be expressed with the following equation [9]:

$$\ln\frac{\lambda_1 I_1}{A_1 g_1} - \ln\frac{\lambda_2 I_2}{A_2 g_2} = \frac{1}{T_{exc}}\frac{(E_1 - E_2)}{k} \qquad (1)$$

Where 1 refers to 460 nm filter and 2 refers to 500 nm filter. g_1 and g_2 are statistical weight at 460 nm and 500 nm respectively. A is the transition probability. While E_1 and E_2 are excitation energy of upper level for the 460 nm and 500 nm spectrum line respectively. λ_1 and λ_2 are wavelength of 460 and 500 nm's spectral lines respectively. I_1 and I_2 are the spectral line intensities which corresponded to each filter used in this work

The electronic excitation temperature (kT_{exc}) can be obtained using equation (1) as follows:

$$kT_{exc} = \frac{(E_1 - E_2)}{\ln\left(\frac{g_2 A_2 \lambda_1 I_1}{g_1 A_1 \lambda_2 I_2}\right)}(eV) \qquad (2)$$

Figure 2 (a, b) shows the variation of peak-to peak luminous intensity of radiation emission from N_2 gas and Air plasma jet respectively using the two filters (460 and 500 nm wavelength) as a function of gas flow rate.

Figure 2 (a) illustrates that for N_2 gas with 460 nm wavelength filter, the peak-to-peak intensity of luminous radiation increases from 60 to 265 a.u. with increasing of the N_2gas flow rate from 3 to 15 L/min, afterwards it decreases from 265 to 115 a.u. with increasing of the N_2 gas flow rate from 15 to 25 L/min. While with 500 nm wavelength filter, it increases from 76 to 258 a.u. with increasing of the N_2gas flow rate from 3 to 12 L/min, and it decreases from 258 to 107 a.u. with increasing of the N_2gas flow rate from 12 to 25 L/min.

Figure 2 (b) illustrates that for Air plasma jet with 460 nm wavelength filter, the peak-to-peak intensity of luminous radiation increases from 8.1 to 16.9 a.u. with increasing the Air flow rate from3 to 12 L/min, afterwards it decreases from 16.9 to 8.5 a.u. with increasing the Air gas flow rate from 12 to 25 L/min, while with 500 nm wavelength filter, it increases from 7.6 to 15.7 a.u. with increasing of the Air flow rate from 3 to 15 L/min, and it decreases from 15.7 to 9.0 a.u. with increasing of Air gas flow rate from 15 to 25 L/min.

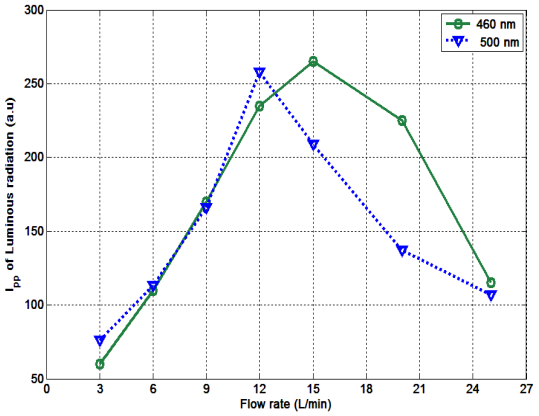

(a)

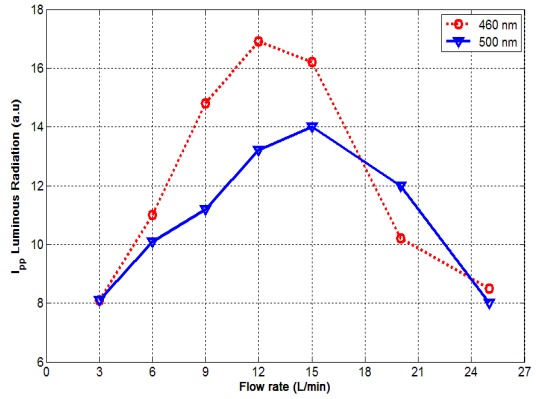

(b)

Fig. 2 The peak-to peak intensity (I_{pp}) of luminous radiation emission from N_2 gas (a) and Air (b) plasma jet versus flow rates for two filters.

Using the spectra atomic data obtained from the National Institute of Standards and Technology, NIST, Atomic spectra database (on-line resources)[10], the parameters (*A*,

g, *E*) in equation 2 are listed in table 1.

Table 1: spectra atomic parameters of filters with wavelengths of 460 nm and 500 nm respectively [10]

Parameter	**460 nm**	**500 nm**
A_{k1} (s^{-1})	2.22 *10^7	1.04 *10^8
g_k	5	7
E_k (eV)	21.159914	23.131852

By substituting the parameters listed in table (1) in equation 2, then the electronic excitation temperature is obtained as a function of N_2 gas and Air flow rates and it plotted as shown in figure 3 (a, b) respectively.

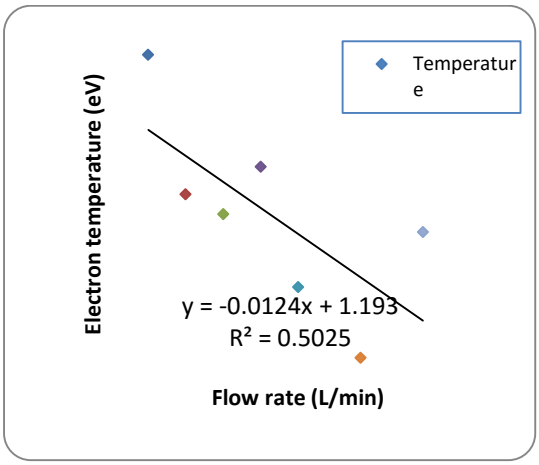

(a)

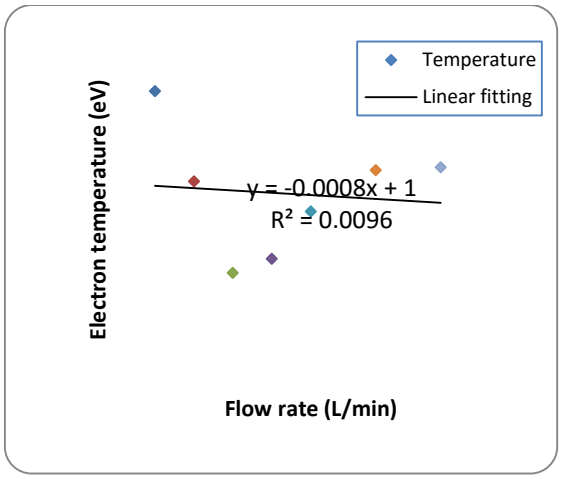

(b)

Fig. 3 (a,b): The estimated electronic excitation temperature versus N_2 gas (a) and Air (b) at different flow rates.

For N_2 gas, figure 3 (a), linear fitting, clears that, KT_{exc} is decreased with increasing of N_2 gas flow rate. Also a linear fitting clears that the rate of change of KT_{exc} with the flow rate, f, is:

$$\left(\frac{dKT_{exc}}{df}\right) = - 0.012407, \text{ and}$$

KT_{exc} is changed in the range from 0.8828 to 1.156 eV i.e., 10240 to 13410 ºK.

For Air, figure 3 (b) clears that, a linear fitting is represented by the following equation:

$$KT_{exc} = -7.5406\times10^{-4}\ f + 1$$

The rate of change of KT_{exc} with Air flow rate, dKT_{exc}/df equals to -7.5406×10^{-4}, figure 3 (b) clears that, KT_{exc} is changed from 0.9977 to 0.9811 eV i.e., 11577 to 11385 ºK. Also, figure 3 (a, b) illustrate that, KT_{exc} is decreased with increasing of the Air and N_2 flow rates respectively (from 3 to 25 L/min).

The above results demonstrate that, the changing of N_2 gas flow rate has more effect on KT_{exc} data than the compressed Air.

3.2 Effect of operation-time on device components temperature

In order to know that the device needs a cooling system or not, the plasma jet device operational time effect on the temperature of the device components such as cathode, envelope and Mylar substrate (with dimensions of (30×10×0.3 mm) needs to be treated has been studied. The temperature of these components is measured by using thermocouple thermometer.

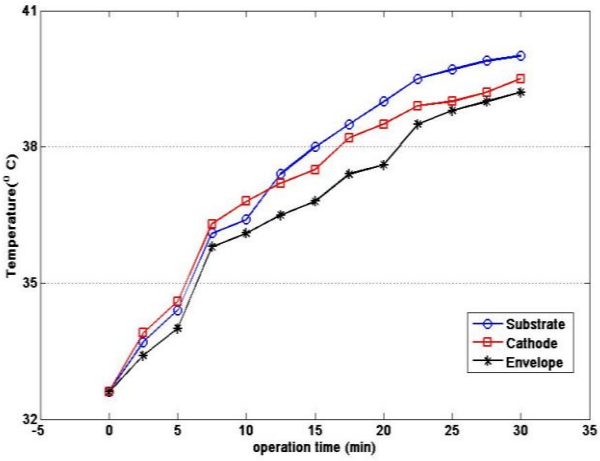

Fig. 4 Cathode, envelope and substrate temperatures of N_2 Plasma Jet at 12 L/min flow rate as a function of the operation time.

Figure 4 and 5 describe the variation of the cathode, envelope and Mylar substrate temperature with the operation time of N_2 gas and Air plasma jet device respectively and at flow rate of 12 L/min. In our case, the original temperature of cathode, envelope and Mylar substrate i.e. at t = 0 equal 32.5 ºC for N_2 gas and 29 ^{0}C for Air (a room temperature during the experimental work time).

Figure 4 clears that, the temperature of the cathode,

envelope and substrate is increased with increasing of the operation time of N_2 gas plasma jet with approximately 6.7-7.5 ^{0}C after 30 min to reach approximately 39.2-40 ^{0}C. Figure 5 shows that the components temperature is increased with increasing of the operation time of Air plasma jet with approximately 7.2-9.8 ^{0}C after 30 min to reach approximately 36.2-38.8 ^{0}C.

Figures 4 and 5 illustrate that a cooling system is not required to cool down the plasma jet device components.

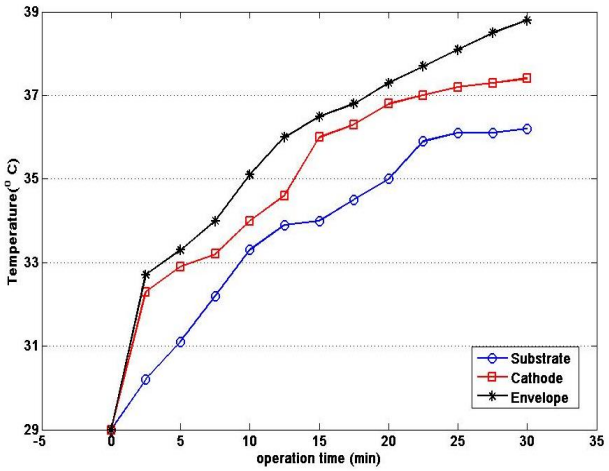

Fig. 5 Cathode, envelope and substrate temperatures of Air Plasma Jet at 12 L/min flow rate as a function of the operation time

3.3 Study of PET surface morphology using SEM before and after treatment with N_2 and Air plasma jet

Scanning electron microscope, SEM, images were taken to visualize the changes in the surface of samples. The SEM images provided a qualitative type of analysis by visualizing the change in the surface of the polymer sample [11]. Surface morphologies of untreated and different treated times of PET polymer surfaces were evaluated by SEM at a magnification of 370X and the operation at electron energy of 5 kV. Also the surface plot of SEM images was detected by using surface plot tool in Image J software. PET samples in our study have dimensions of 30×15 mm with thickness of 19 µm and it is fixed at an axial distance of 5.5 mm from the cathode surface. Figure 6 (a) shows the SEM image of untreated PET polymer surface while figure 6 (b) shows the surface plot of this SEM image.

Figures 7 and 8 show the surface plot of the SEM image after 2.5 min, 5 min, 7.5 min, 10 min and 15 min for N_2 and Air plasma jet at a flow rate of 12 L/min treatment of PET polymer surfaces respectively.

As shown in figure 6 and 7, the surfaces are relatively smooth with some contaminants especially in figure 6 b, 7 c and e. Moreover, these surface plots of SEM images reveal significant differences between before and after plasma treatment, indicating that there was roughness occurred to the PET polymer surface after N_2 plasma jet treatment. This roughness layer of the PET surface is observed after 2.5 and 7.5 min treatment while approximately removal of this roughness layer on the PET surface is observed after 5 and 10 min treatment of N_2 plasma jet while there is less surface roughness after 15 min treatment time.

(a)

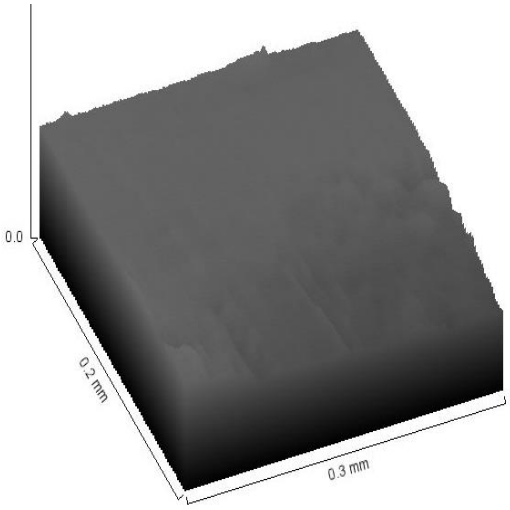

(b)

Fig. 6 (a) SEM image (b) the surface plot for untreated PET polymer surface.

The surface plot shown in figures 6 and 8 reveal a significant difference between the un-treated and treated samples, indicating that there was roughness occurred to the PET polymer surface after Air plasma treatment especially after 5, 7.5, 10 and 15 min. Finally, it can be seen that, for N_2 plasma jet treatment, a roughness layer is detected after 2.5, 7.5 min while, for Air plasma jet, a roughness surface layer is detected after 5 and 10 min. A removal of this roughness layer is detected after 5, 10 and 15 min treatment time in the case of N_2 plasma jet while a less removal of roughness is detected after 7.5 and 15 min treatment time in the case of Air plasma jet.

4 Conclusion

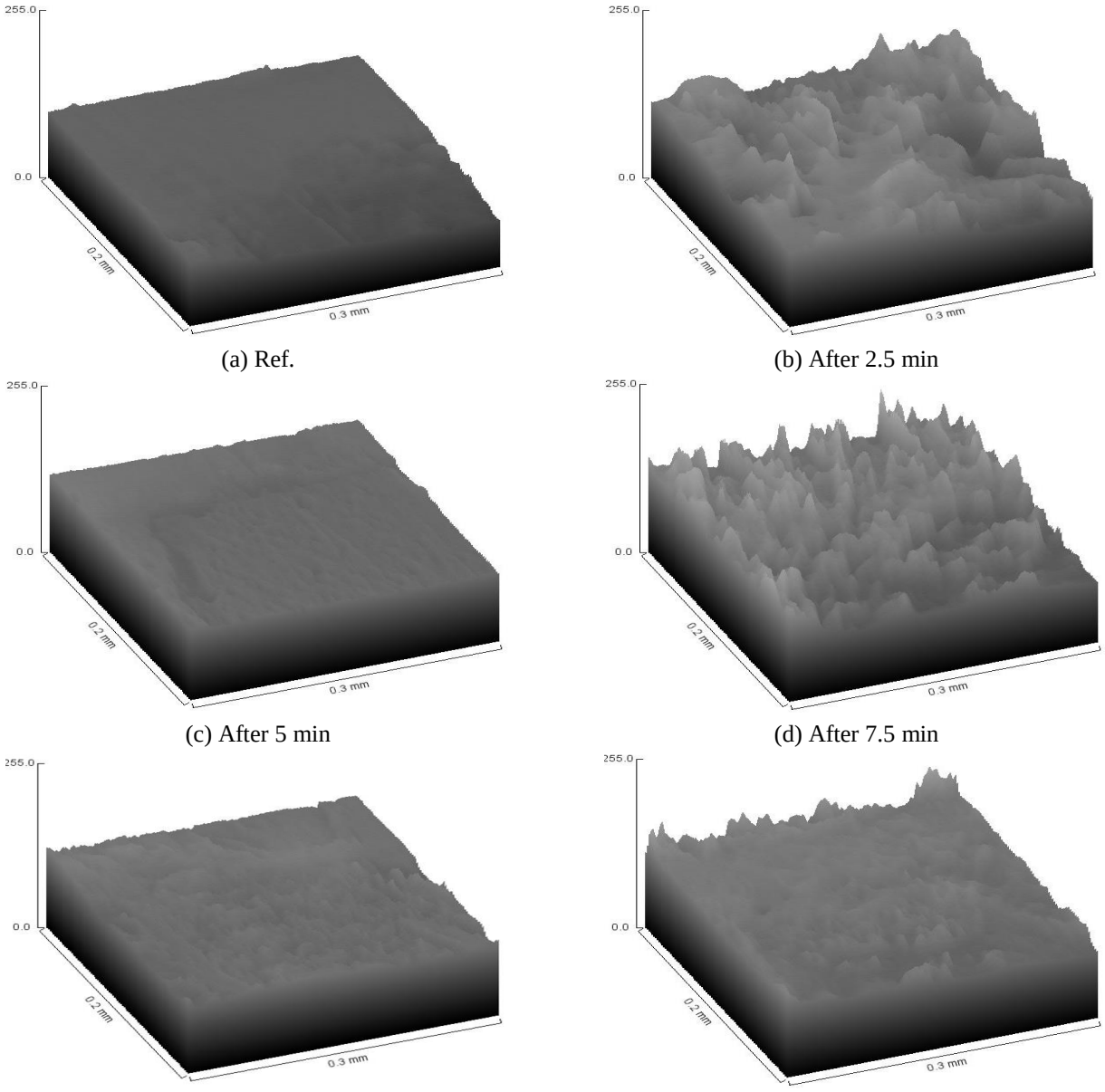

(a) Ref. (b) After 2.5 min

(c) After 5 min (d) After 7.5 min

(e) After 10 min (f) After 15 min

Fig. 7: Surface plot of SEM images of PET surface before treatment and after 2.5, 5, 7.5, 10 and 15 min N_2 plasma jet treatment.

Results of linear fitting distribution of electronic excitation temperature, $KT_{exc.}$ with N_2 and compressed Air flow rates confirmed that, $KT_{exc.}$ for N_2 is greater than that for compressed Air, and for both of them $KT_{exc.}$ is decreased with increasing of flow rate. At N_2 flow rate of 12 L/min, KT_{exc} = 1.044 eV= 12110 ºK while for Air plasma jet it is 0.9909 eV=11500 ºK.

From the measurements of the effect of the operational time of the device component's temperature, it can be concluded that no external cooling required for both N_2 and Air plasma jet device.

Detection of the surface roughness of the treated PET polymer sample with N_2 and compressed Air at different treatment times cleared that, the surface roughness is detected clearly for most treatment time under consideration (t = 5, 7.5, 10 and 15 min) for compressed Air, while for N_2 gas it detected approximately at t = 2.5 and 7.5 min. These results may be attributed to electronic excitation temperature data for N_2 gas and compressed Air.

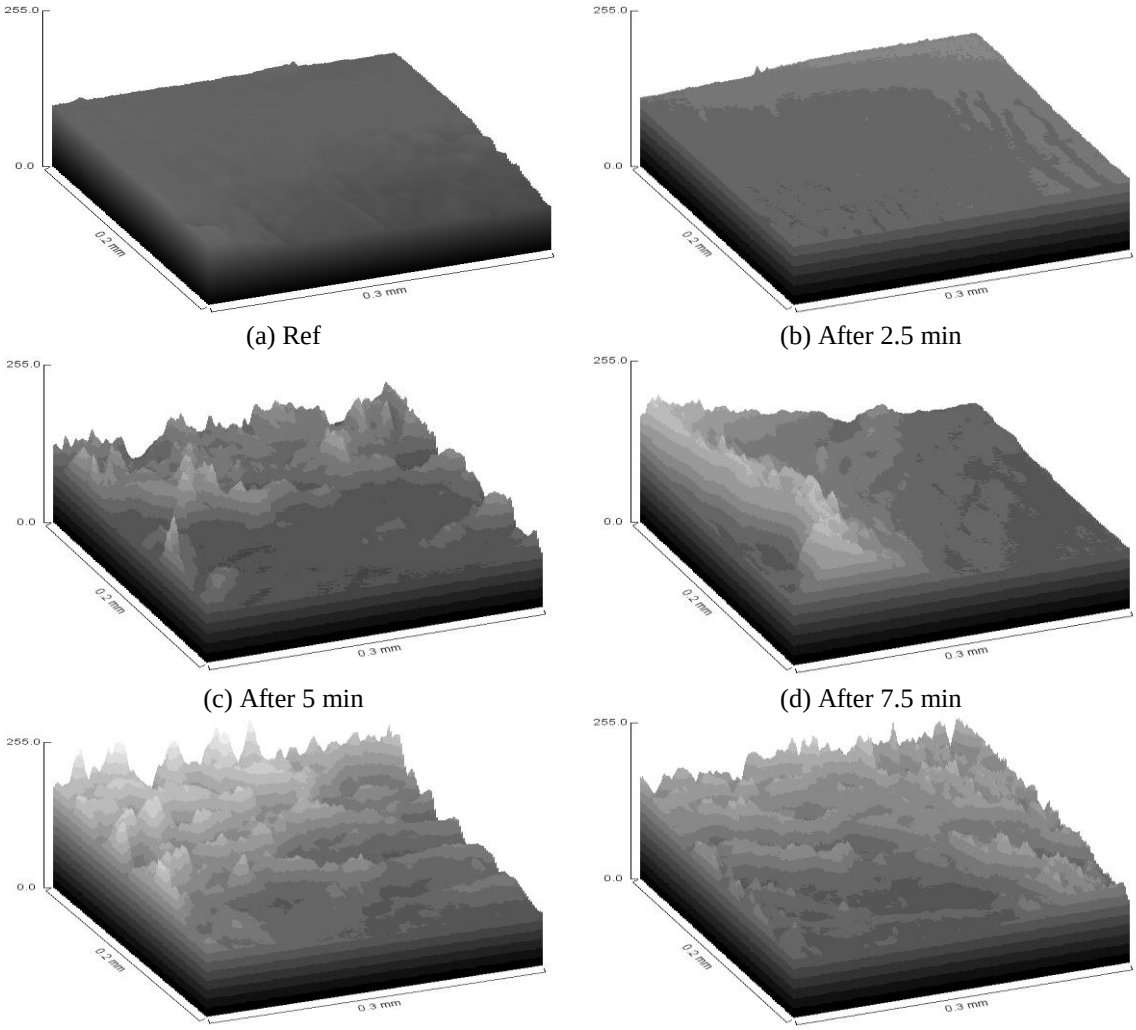

(a) Ref (b) After 2.5 min

(c) After 5 min (d) After 7.5 min

(e) After 10 min (f) After 15 min

Fig. 8: Surface plot of SEM images of PET surface before treatment and after 2.5, 5, 7.5, 10 and 15 min Air plasma jet treatment.

References

[1] S.D. Anghel, A. Simon, M.A. Papiu, O.E. Dinu "A Very Low Temperature Atmospheric-Pressure Plasma Jet in a Single Electrode Configuration" Rom. Journ. Phys., Vol. 56, Supplement, P 90 – 94 Bucharest, (2011).

[2] C. Tendero, C. Tixier, P. Tristant, J. Desmaison, P. Leprine, Atmospheric Pressure Plasmas: a review, Spectrochim. Acta Part b 61, 2 -30 (2006).

[3] B. Eliasson, U. Kogelschaty, IEEE Trans, Plasma Sci, 19, 303 (1991).

[4] R. Dorai, M.J. Kushner, J. Phys. D: Appl. Phys. 36, 666 (2003).

[5] M. Laroussi, IEEE Trans. Plasma Sci. 24, 1188, (1996).

[6] M. Laroussi, Plasma Proc. Polym. 2, 391 (2005).

[7] K.M. Ahmed, T.M. Allam, H.A. El-sayed, H.M. Soliman, S.A. Ward and E.M. Saied, "Design, Construction and Characterization of AC Atmospheric Pressure Air Non-Thermal Plasma Jet", Journal of Fusion Energy, vol.33, issue 6, P 627 – 633, (2014).

[8] T.M. Allam, S.A. Ward, H.A. El-sayed, E.M. Saied, H.M. Soliman, and K. M. Ahmed "Electrical Parameters Investigation and Zero Flow Rate of Nitrogen Atmospheric Nonthermal Plasma Jet ", EPE, vol. 6, no. 12, P 437 – 448, (2014).

[9] T. D. Hahn and W. L. Wiese, "Atomic transition probability ratio between some Ar I 4s-4p and 4s-5p transitions," Physical Review A, vol. 42, no. 9, pp. 5747-5749, 1990.

[10] NIST Atomic Spectra Database Lines Data on. [Online]. http://physics.nist.gov\

[11] H. Mohandas, G. Sivakumar, P. Kasi, S. K. Jaganathan, and E. Supriyanto, "Microwave-Assisted Surface Modification of Metallocene Polyethylene for Improving Blood Compatibility," *BioMed Research International*, vol. 2013, pp. Article ID 253473, 7 pages, 2013.